Analysis of Transient Magnetic Shielding made by Conductive Plates with a PEEC method

Y. Du and Hongcai Chen

The Hong Kong Polytechnic University, Department of Building Services Engineering, Hung Hom, Kowloon, Hong Kong

***Abstract*— This paper analyzed transient magnetic fields generated by the lightning current in the presence of 3D conductive plates. An extended PEEC method was introduced to establish an equivalent circuit with frequency-variant parameters for time-domain simulation. Several techniques were proposed to reduce the computational complexity in the large-plate simulation. These include the analytical function of current density, non-uniform meshing scheme, and vector fitting technique. Numerical and experimental results were presented to validate the proposed method. Good agreements were observed.**

Index Terms— **transient magnetic field, lightning, plate, PEEC.**

I. Introduction

Lightning generates substantial transient electromagnetic fields in buildings, and induces transient voltages and currents in power and signal equipment or systems. Such transients could cause malfunctions, faults or even physical damages to sensitive equipment. Transient electromagnetic fields in buildings are greatly affected by building structures, such as columns, beams, metal decking and other large plates. To provide appropriate protection for the equipment, it is necessary to develop an efficient mean for the evaluation of transient magnetic fields or shielding performance of planar structures.

Electromagnetic shielding is generally addressed analytically and numerically in the frequency domain. Analytical methods are applicable to simple shielding structures possessing 2D geometry or symmetrical properties [1-2]. Recently, significant advances in numerical electromagnetics have been made in providing numerical solutions to shielding problems. Both the boundary element method and the finite element method [3-4] have been successfully applied to address shielding problems in the frequency domain. These methods can deal with complex geometry and material characteristics of conductive bodies.

Recently the partial element equivalent circuit (PEEC) method has been introduced for field or shielding analysis. The uniform meshing model was presented in [5] for a conductive plate at low frequency, and in [6] for magnetic materials in transient field analysis. In these studies, the current density is constant inside a cell. To reach a considerable accuracy, a large full matrix equation needs to be established, and a considerable amount of computational resources be required. In [7] an analytical function was introduced to represent the current distribution across the plate thickness at low frequency. A two-dimensional meshing scheme would then is sufficient for modeling 3D plates. This significantly reduces the number of unknown variables in solving such field problems. A transient analysis of magnetic fields associated with thin layers was also presented in [8]. As the 1D diffusion equation was applied, this approach is limited to the problems with 2D geometry only.

This paper introduces an extended PEEC method for analyzing transient magnetic fields generated by a lightning discharge current in the presence of three-dimensional conductive plates. The plates are modeled as a set of interconnected and coupled circuit components. The current within the plate is solved with a circuit analysis technique, subsequently the transient magnetic fields around the plates with the Bio-Savart law. In this paper several techniques are proposed to reduce the computation complexity in the large-plate simulation. These include the analytical function of current density, non-uniform meshing scheme, and vector fitting technique. Numerical results of the magnetic fields in testing cases are presented, and are compared with the frequency-domain results obtained from the finite-element-method. A laboratory experiment is introduced finally for validating the proposed method in calculating transient magnetic fields.

II. Equivalent Circuit Model of Plates

The problem under investigation consists of a conductive plate excited by an external source associated with a lightning discharge current, as shown in Fig.1(a). The plate is made from linear non-ferromagnetic material, and has a conductivity of σ and permeability of μ_0. Note that plate thickness d is very small, compared with its surface dimensions. The induced current, therefore, is negligible in the z direction, and flows in the x-y plane only.

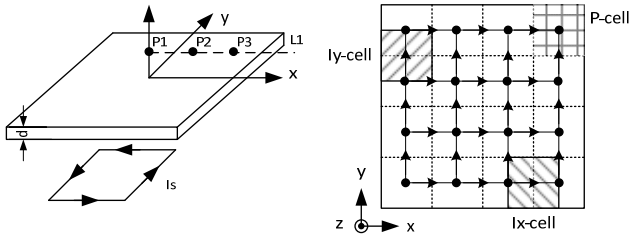

Fig.1 Conductive plate for transient field analysis

A. Grid generation

In order to solve for the induced current numerically, the plate is divided into a number of cuboids called voltage cells over its planar surface, as shown in Fig.1(b). Current cells are formed by taking the volume between the centers of adjacent voltage cells. The current cells are classified into two types: *x-dir.* cells and *y-dir.* cells, which carry the currents in these two orthogonal directions, as shown in Fig. 1(b). In each current cell, the current density is uniform on the x-y plane, but varies along the plate thickness. Current density across the plate thickness can be described with an analytical function given in Section II(*B*).

It is known that the induced current in the plate is unevenly distributed over its planar surface due to skin effect. To solve the problem efficiently a non-uniform meshing scheme is proposed. In this scheme, the plate is divided into a number of identical small voltage cells (elements) first. In Fig. 2(a), the grey squares represent the voltage elements, and the black dots represent the element centers. If the current in a local area does not change significantly, voltage elements in this area are merged into a bigger cell, as illustrated in Fig.2(b). The current cells then are generated from adjacent merged voltage cells. Each merged current cell consists of a number of basic current cells (current elements). Fig. 2(c) and 2(d) illustrate some of generated *x-dir*. cells and *y-dir*. current cells. Both *i* and *j* in Fig.2(a) denote the row and column indices of an element.

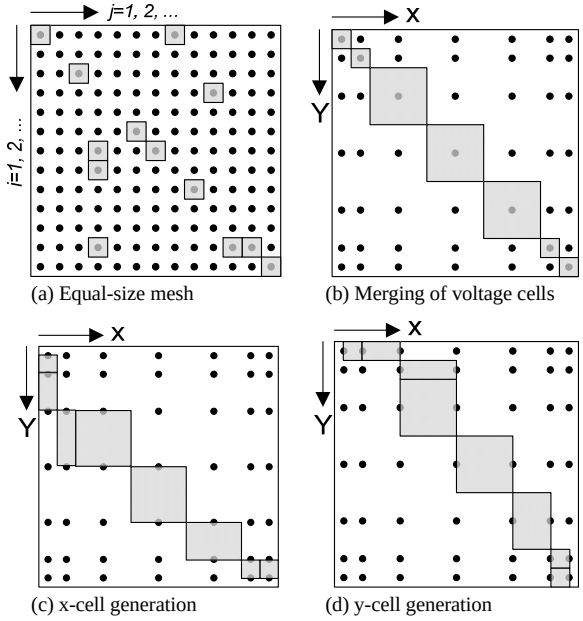

(a) Equal-size mesh (b) Merging of voltage cells

(c) x-cell generation (d) y-cell generation

Fig.2 Non-uniform meshing scheme

Consider a plate with $n \times n$ current elements. Impedance matrix $Z_e = \{z_{ij}^e\}_{n\times n}$ for current elements can be established. z_{ij}^e represents the impedance between the reference element (row 1 and column 1) and the element in row *i* and column *j* on the plate. Note that the sizes of all elements are identical. Mutual impedance of two elements is determined by their relative positions in the plate, and can be obtained from impedance matrix Z_e. Circuit parameters of merged current cells can then be constructed with matrix Z_e directly. For example, mutual impedance of two cells is obtained by adding mutual impedance among elements in these two cells, then dividing the result by the element numbers of these cells in the direction transverse to the current. Assume two *x-dir*. cells *a* and *b* have respectively elements in row i_a $(i_{a1} \cdots i_{a2})$, i_b $(i_{b1} \cdots i_{b2})$, and column j_a $(j_{a1} \cdots j_{a2})$, j_b $(j_{b1} \cdots j_{b2})$, mutual impedance z_{ab}^c of these two cells is expressed by

$$z_{ab}^c = \frac{\sum_{j_b=j_{b1}}^{j_{b2}} \sum_{j_a=j_{a1}}^{j_{a2}} \sum_{i_b=i_{b1}}^{i_{b2}} \sum_{i_a=i_{a1}}^{i_{a2}} z^e_{|i_a-i_b|+1,\,|j_a-j_b|+1}}{(j_{a2}-j_{a1}+1)(j_{b2}-j_{b1}+1)} \tag{1}$$

Now consider to build impedance matrix $Z_c = \{z_{ij}^c\}_{m^2\times m^2}$ for $m \times m$ merged cells without using Z_e. The computational complexity would be greater if $m > \sqrt{n}$, and will be significantly increased when *m* approaches *n*.

B. Equivalent circuit model

The equation for magnetic vector potential $A(r)$ and electric scalar potential (voltage) $\phi(r)$ enforced at point *r* on a plate is given by:

$$-\nabla\phi(r) = \frac{J(r)}{\sigma} + j\omega A(r) \tag{2}$$

where ω is the angular frequency of the exciting current, and $J(r)$ is the current density in the plate. Vector potential $A(r)$ is contributed by both induced current in the plate and external source current I_s, and is expressed by

$$A(r) = \frac{\mu_0}{4\pi}\int_{v'}\frac{J(r')}{|r-r'|}dv' + \frac{\mu_0}{4\pi}\int_{l'}\frac{I_s}{|r-r'|}dl' \tag{3}$$

In current cell *i*, current density $J_i(z)$ varies along the *z* direction only. It can be expressed approximately by an analytical function [7], as follows:

$$J_i(z) = J_i^+ e^{\alpha(z-z_0)} + J_i^- e^{-\alpha(z-z_0)} \tag{4}$$

where J_i^- and J_i^+ are respectively the current densities on the upper and lower surfaces of the cell. In (4) $\alpha = \sqrt{-\omega\mu_0\sigma}$ and z_0 is the position of the middle *x-y* plane of the cell. Total cell current I_i can then be obtained by integrating (4) over its cross-section area, as follow:

$$I_i = s_i J_i^+ + s_i J_i^- = I_i^+ + I_i^- \tag{5}$$

where effective cross-sectional area $s_i = 0.5w\cdot\sinh(\alpha d)/\alpha$, and *w* is the cell width. Both I_i^- and I_i^+ are the currents associated with the upper and lower cell surfaces.

Integrating (2) along a line segment on both upper and lower surfaces of cell *i* yields two integral equations, as follows:

$$\begin{aligned}\Delta V_i^+ = {} & \frac{\Delta l_i}{\sigma}J_i^+ + \frac{\Delta l_i}{\sigma}J_i^- + \frac{j\omega\mu_0}{4\pi}\sum_{j=1}^{N_c}\int_{l_i}\int_{\Omega_j'}\frac{J_j(z')}{|r^+-r'|}d\Omega' dl \\ & + \frac{j\omega\mu_0}{4\pi}\sum_{j=1}^{N_s} I_{sj}\int_{l_i}\int_{l_{sj}'}\frac{1}{|r^+-r'|}dl' dl\end{aligned} \tag{6a}$$

$$\begin{aligned}\Delta V_i^- = {} & \frac{\Delta l_i}{\sigma}J_i^+ + \frac{\Delta l_i}{\sigma}J_i^- + \frac{j\omega\mu_0}{4\pi}\sum_{j=1}^{N_c}\int_{l_i}\int_{\Omega_j'}\frac{J_j(z')}{|r^--r'|}d\Omega' dl \\ & + \frac{j\omega\mu_0}{4\pi}\sum_{j=1}^{N_s} I_{sj}\int_{l_i}\int_{l_{sj}'}\frac{1}{|r^--r'|}dl' dl\end{aligned} \tag{6b}$$

where r^+ and r^- are respectively the positions of observation points in the integrand on the upper and lower surfaces. Both N_c and N_s are respectively the numbers of plate cells and source wires. (6) can be further transformed into two circuit equations using cell currents I_j^+ and I_j^-, and source current I_{sj}, as follows:

$$\begin{aligned}\Delta V_i^- &= R_i^{-+}I_i^+ + R_i^{--}I_i^- + \sum_{j=1}^{N_c} j\omega(L_{ij}^{-+}I_j^+ + L_{ij}^{--}I_j^-) + \sum_{j=1}^{N_s} j\omega L_{ij}^{s-}I_{sj} \\ \Delta V_i^+ &= R_i^{++}I_i^+ + R_i^{+-}I_i^- + \sum_{j=1}^{N_c} j\omega(L_{ij}^{++}I_j^+ + L_{ij}^{+-}I_j^-) + \sum_{j=1}^{N_s} j\omega L_{ij}^{s+}I_{sj}\end{aligned} \tag{7}$$

where R_{ij}^{pq} and L_{ij}^{pq} $(p, q = "+" \text{ or } "-")$ are respectively the mutual resistance and inductance between the upper and lower surfaces in cells *i* and *j*, and L_{ij}^{sp} is the inductance associated with the source current wires. They are expressed by

$$R_i^{pq} = \frac{\Delta l_i}{\sigma\Delta s_i}\cdot e^{\frac{p\cdot q\cdot\alpha\cdot d}{2}} \tag{8a}$$

$$L_{ij}^{pq} = \frac{\mu_0}{4\pi\Delta s_j}\int_{l_i}\int_{\Omega_j'}\frac{e^{q\cdot\alpha(z'-z_0)}}{\sqrt{\Delta x^2+\Delta y^2+(z^p-z')^2}}d\Omega' dl \quad (8b)$$

$$L_{ij}^{sp} = \frac{\mu_0}{4\pi}\int_{l_i}\int_{l_{sj}'}\frac{1}{\sqrt{\Delta x^2+\Delta y^2+(z^p-z')^2}}dl' dl \quad (8c)$$

and z^p ($p = "+"$ or $"-"$) is the coordinate of the upper or lower cell surface in the *z* direction. (7) and (8) are applicable to both *x-dir.* and *y-dir.* current cells.

It is noted from (6) that voltage in a current cell is balanced by resistive and inductive voltages generated by the current in its cell, and inductive voltage generated by other cells. In cell *i* both V_i^+ and V_i^- remain the same as there is no *z-dir*. current. An equivalent circuit for cell *i* then is established, as shown in Fig.3.

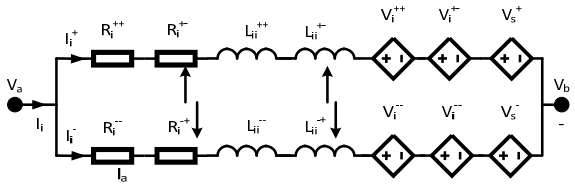

Fig. 3 Equivalent circuit of a current cell

In Fig. 3, $V_{i,\Sigma}^{pq}$ and $V_{si,\Sigma}^{p}$ represent the inductive voltages contributed by currents in other cells and source currents, respectively. The vertical arrow means the resistive or indurative voltage controlled by the current in the opposite surface. According to the topology of voltage and current cells, this branch is connected to other branches at voltage cells *a* and *b*. Therefore, an equivalent circuit network, which consists of a number of interconnected and coupled branches, is formulated.

III. Time Domain Implementation

It is noted from (8) that circuit parameters of the equivalent circuit are generally frequency-dependent. Further investigation into (8) reveals that self impedance of a cell varies with frequency significantly, while mutual inductance between cells or between cells and source wires generally does not.

In order to perform the transient analysis in the time domain, the frequency-dependent network has to be converted into a modified circuit with frequency–invariant parameters. This can be possibly done with a curve fitting technique [9]. For example, self impedance $Z_{ii}^{pq} = R_{ii}^{pq} + sL_{ii}^{pq}$ of cell *i* in *s*-domain is expressed approximately by

$$Z_{ii}^{pq}(s) = R_0^{pq} + sL_0^{pq} + \sum_{k=1}^{M}\frac{s}{s+R_k^{pq}/L_k^{pq}}\cdot R_k^{pq} \quad (9)$$

After all the poles are identified this rational function can be realized with an equivalent cascade circuit consisting of frequency-invariant resistors R_k^{pq} and inductors L_k^{pq}, as shown in Fig. 4. Now the plate is represented by an extended network with frequency-invariant parameters. Time-domain network equations can be established using any circuit analysis approach including a modified nodal analysis approach.

For numerical solution, a discretization scheme with the backward Euler method is employed to generate a time discrete solver. In order to reduce the size of network matrix, this discretization scheme is applied directly to convert the cascade RL circuit shown in Fig.4 into a time discrete equation. This discretion equation then is integrated into the time discrete solver for the network. Fig. 4 (c) shows the time discrete equivalent circuit for a parallel RL circuit. Its time discrete equation is expressed by

$$V_k^{pq}[n] = R_{eq,k}^{pq}\cdot I_k^{pq}[n] - V_{eq,k}^{pq}[n] \quad (10)$$

where

$$R_{eq,k}^{pq} = \frac{R_k^{pq}\cdot L_k^{pq}/\Delta T}{R_k^{pq}+L_k^{pq}/\Delta T}$$

$$V_{eq,k}^{pq}[n] = R_{eq,k}^{pq}\cdot I_k[n-1] - R_{eq,k}^{pq}/R_k^{pq}\cdot V_{eq,k}^{pq}[n-1]$$

For the cascade RL circuit shown in Fig. 4(a), the time discrete equation is given by

$$V^{pq}[n] = (\sum_{k=1}^{M} R_{eq,k}^{pq})\cdot I^{pq}[n] - \sum_{k=1}^{M} V_{eq,k}^{pq}[n] \quad (11)$$

where *M* is the number of parallel RL circuits. The timer-domain current density in the plate can then be obtained numerically.

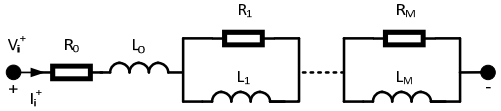

(a) Equivalent circuit for Z_{ii}^{++}

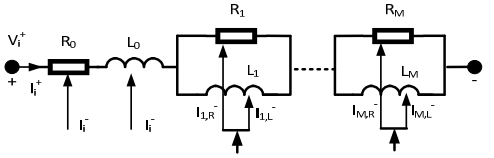

(b) Equivalent circuit for Z_{ii}^{+-}

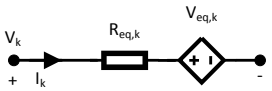

(c) Time discrete equivalent circuit of a parallel *RL* circuit

Fig. 4 Equivalent circuit of frequency-dependent impedance

IV. Numerical and Experimental Results

The proposed method has been implemented on the platform of MATLAB, and been applied to solve transient magnetic fields in the presence of conductive plates. The results are compared with numerical results calculated with a commercial FEM software package in the frequency domain, and time-domain measurement results obtained in the laboratory experiment.

Fig. 1(a) shows the configuration of a model under the evaluation. In this model, an aluminum plate is excited by an external magnetic field generated from a wire loop underneath. The aluminum plate has the conductivity of $\sigma = 3.75\times10^7$ S/m, and the dimensions of 400×400×2mm^3. The square loop is located at the distance of 200mm from the plate, and has a side length of 200mm. It carries either an AC current or an impulse current similar to the lightning discharge current. The magnetic fields along a horizontal line (L1) are evaluated, which is 200mm above the plate as shown in Fig. 1(b). The non-uniform meshing scheme described in Section II is applied. The plate is divided into 100×100 identical voltage elements. After merging some of elements, the cell number is reduced to 39×39.

Fig.5 shows the calculated magnetic field along the measurement line (L1) in the frequency range from 50Hz to 50kHz. The source current has the magnitude of 1A. Note that the 1st lightning return stroke current has a representative waveform of 10/350μs. The primary spectrum of lightning current is covered in this frequency range. The simulation results using the FEM method are also presented in the figure. It is found that these results match generally, and the difference is less than 3%. The computation time is 16 h 27 sec. on a

workstation (Inter®Xeon 2xCPU E5-2650 V3 @ 2.3GHz) with the FEM method, and is 34 min. 25 sec. on a PC (Inter@Core™ i7-2600 CPU @ 3.4GHz) with the proposed method.

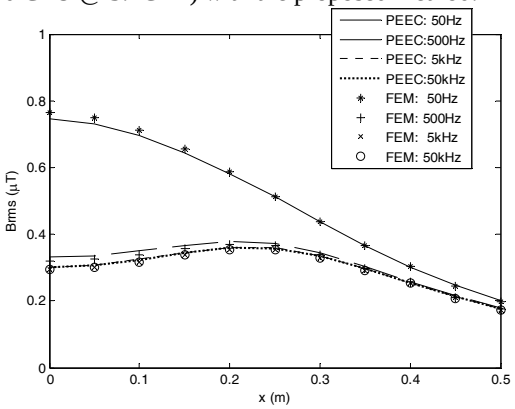

Fig. 5 Magnetic fields along Line L1 in the frequency range of 50Hz-50kHz

Transient magnetic field along the line was calculated as well. To validate the simulation results, a laboratory experiment was carried out. The wire loop made with a 10-turn coil was connected to a combination wave generator. The transient magnetic field was measured with a tailor-made search coil. This 1000-turn coil has the diameter of 45mm and height of 35mm. It is loaded with a 3.8 ohm resistor. The calibration was conducted by placing the search coil in the center of a 1 m x 1 m square loop. Both current in the square loop and voltage on the coil were measured with Techtronic MDO3054 and Pearson CT4977. Fig. 6 shows the normalized current and voltage in the calibration. It is found that both curves match well under the surge waveform. The coil voltage can then represent the surge current. Note that the transient magnetic field is linearly proportional to the surge current. The magnetic field can be obtained with measured coil voltage V_{coil} using the formula of $B = 3.625 \times 10^2 V_{coil}$ μT after the calibration.

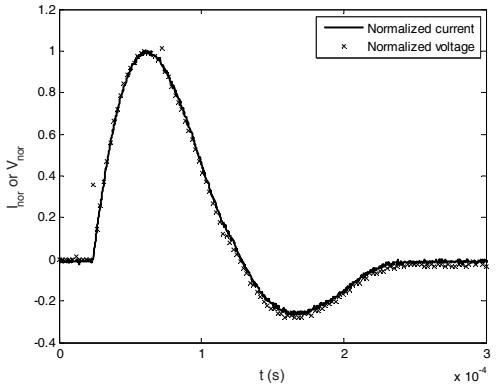

Fig. 6 Measured impulse current in the loop and impulse voltage on the coil

In the validation experiment, the 10-turn wire loop carried an impulse current with the peak value of 327A generated from the combination wave generator. Magnetic field B_z in the z direction was measured with the search coil at three points on L1, as shwon in Fig. 1(a). The surge current was recorded by the MDO3054 and was loaded into the matlab rouitne as an input to calculate the transient magnetic field in the prsence of the plate. Both measured and computed time-domian waveforms are presented in Fig. 7. It is found that these waveforms match well, and the difference of peak values is generally less than 5%. The computation time for 1334 time steps is 37 min 17 sec. on the PC.

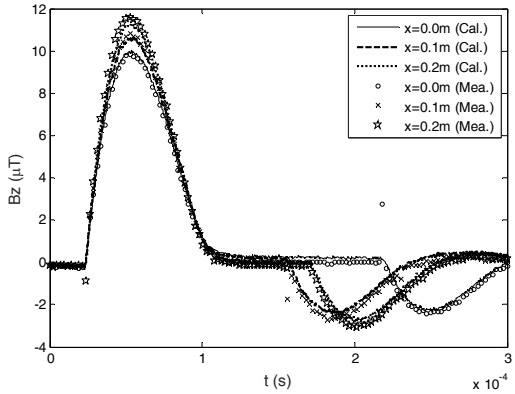

Fig.7 Comparison between calculated and measured transient results

V. Conclusions

This paper presented an equivalent circuit method for analyzing lightning–induced magnetic fields in the presence of conductive plates. In this method, an analytical function was introduced to deal with eddy current across plate thickness, and a non-uniform meshing scheme was proposed to reduce computational complexity. To perform the time-domain simulation in a network with frequency variant parameters, the vector-fitting technique was applied. This proposed method has been validated in the frequency domain using the results obtained from the BEM. An experiment has been conducted as well, and the proposed method in calculating transient magnetic fields generated by the lightning current has been validated.

Acknowledgment

The work was supported by a grant from the Research Grants Council of HKSAR (Project No. 514813 & 15203815).

References

[1] L. Hasselgren and J. Luomi, “Geometrical aspects of magnetic shielding at extremely low frequencies,” *IEEE Trans. on EMC*, vol. 37, no. 3, pp. 409–420, Aug. 1995.

[2] Y. Du, T.C. Cheng and A.S. Farag, “Principles of power-frequency magnetic field shielding with flat sheets in a source of long conductors,” *IEEE Trans on EMC*, Vol. 38, No. 3, Aug. 1996 pp. 450–459

[3] L. Hasselgreen, E. Moller, and Y. Hamnerius, "Calculation of magnetic shielding of a substation at power frequency using FEM," IEEE Trans, on Power Delivery, vol. 9, pp. 1398-1405, July 1994.

[4] Y. Du and J. Burnett, “ELF shielding performance of metallic enclosure for heavy-current conductors,” IEE Proc. – Gener. Transm. Distrib. Vol. 146, No. 3, May 1999, pp. 223-228.

[5] A. Canova, G. Gruosso, and M. Repetto, “Integral methods for analysis and design of low-frequency conductive shields,” *IEEE Trans. Magn.*, vol. 39, no. 4, pp. 2009–2017, Jul. 2003.

[6] D. Romano and G. Antonini, “Augmented Quasi-Static Partial Element Equivalent Circuit Models for Transient Analysis of Lossy and Dispersive Magnetic Materials,” DOI: 10.1109/TMAG.2015.2507998

[7] Y. Du, Q. B. Zhou, and X. H Wang, “Equivalent Circuit Approach for Evaluating Low-Frequency Magnetic Fields in the Presence of Non-Ferromagnetic Plates,” *IEEE Trans. Magn.*, vol. 45, no. 3, pp. 960–963.

[8] O. Bottauscio, M. Chiampi and a. Manzin, “Transient Analysis of Thin Layers for the Magnetic Field Shielding,” *IEEE Trans. on Magnetics*, vol. 42, no. 4, April 2006, pp. 871-874

[9] B. Gustavsen, "Fast passivity enforcement for pole-residue models by perturbation of residue matrix eigenvalues," *IEEE Trans. on PWRD*, vol. 23, pp. 2278-2285, 2008.